

# Electrode-Electrolyte Interface Model of Tripolar Concentric Ring Electrode and Electrode Paste

Seyed Hadi Nasrollahhosseini, *Member, IEEE*, Preston Steele, and Walter G. Besio, *SeniorMember, IEEE*

**Abstract**—Electrodes are used to transform ionic currents to electrical currents in biological systems. Modeling the electrode-electrolyte interface could help to optimize the performance of the electrode interface to achieve higher signal to noise ratios. There are previous reports of accurate models for single-element biomedical electrodes. In this paper we develop a model for the electrode-electrolyte interface for tripolar concentric ring electrodes (TCRE) that are used to record brain signals.

## I. INTRODUCTION

Physiological systems such as the cardiovascular system, nervous system, and muscular system all generate ionic current flows in the body. Each physiological process is associated with specific signals that reflect the underlying nature and activities of each source. One such physiological signal of interest is the electroencephalography (EEG) which is the recording of brain electrical activity.

Biomedical signals can be obtained with electrodes that sense the variations in electrical potential generated by physiological processes. Electrodes convert the ionic currents flowing in the body generated by underlying cells into electrical currents [1]. Therefore, electrodes transduce ionic currents, in our case from the human body into electrical currents.

A mathematical model of the electrode, electrolyte, and body may help us to have a better understanding of how biomedical signals are obtained by electrodes. Since electrodes act as transducers, we need to understand the mechanisms that generate the transduction process between the electrode and the human body. Moreover, physiological processes in the human body generate ionic current flows in the volume conductor, the body. Hence, at the contact site of an electrode to the body an electrode-electrolyte interface forms. Figure 1 shows the contact of an electrode to an electrolyte. At the interface of electrode-electrolyte, chemical reactions take place that can be shown by the following equations [2]:



\*Research supported by NSF award 1539068 to WB. The content is solely the responsibility of the authors and does not necessarily represent the official views of the National Science Foundation.

S. H. Nasrollahhosseini is with the Electrical, Computer, and Biomedical Engineering Department, University of Rhode Island, Kingston, RI02881 USA, (e-mail: hadi@ele.uri.edu).

P. Steele is with CREmedical Corp., Kingston, RI 02881 USA, (email: preston@cremedical.com)

W. G. Besio is with the Electrical, Computer, and Biomedical Engineering Department, University of Rhode Island, Kingston, RI02881 USA, (e-mail: besio@uri.edu).

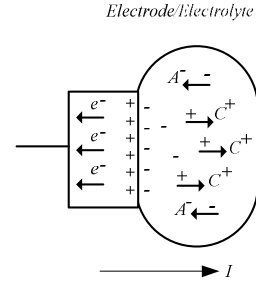


Figure 1: Electrode-electrolyte interface



There are some considerations regarding the above equations and the electrode-electrolyte interface. First of all, Equation (1) shows the oxidation reaction from left to right, and the reduction reaction from right to left, and both reduction and oxidation can occur at the electrode-electrolyte interface. Secondly, Equation (1) shows that for current-ion exchange at the interface, we should place a metal (C) into an aqueous solution containing ions of the metal (C+). Thus, there is oxidation and cations are dispersed into the electrolyte and electrons are left in the electrode. Equation (2) shows that the anions (A) can also be oxidized to a neutral atom and release one or more electrons by moving to the interface.

Obtaining an accurate model for the electrode-electrolyte interface is complicated and has been studied for many years. The concept of the electric double layer was first proposed by Helmholtz in 1879 [3]. He found that at the electrode-electrolyte interface, since the electrolyte is saturated with charged electrons, the ions with the same charges will be pushed back while the opposite charges will be attracted. Therefore, at the electrode-electrolyte interface there will be two compact layers of opposite charges called the “electric double layer” (EDL).

In 1899 Warburg proposed the first electrode-electrolyte model. He proposed a series combination of a capacitor and resistor in which the magnitude of the reactance and resistance is dependent on the electrode type, area (including surface conduction), the electrolyte, the frequency, and the current density [4]. In the Warburg model  $R_w$  and  $C_w$ , were proposed for infinitely low density current, which decreases by the square root of frequency as the frequency increase ( $\frac{1}{\sqrt{f}}$ ). This model is depicted in Fig. 2a.

In 1932 Fricke proposed a similar model for the electrode-electrolyte interface with the Warburg combination

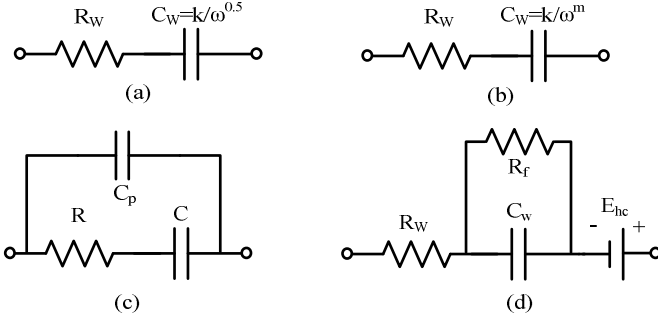


Figure 2: Electrical circuit model evolution of the electrode-electrolyte interface. (a) Warburg, (b) Fricke (c) Randles, and (d) Geddes and Baker models

of series resistor and capacitor, adding that  $C_w = \frac{k}{\omega^m}$ . So in the proposed Fricke model which is shown in Fig. 2b the Warburg reactance and resistance are as follows:

$$X_w = \frac{1}{k\omega^{1-m}} \quad (3)$$

$$R_w = \frac{X_w}{\tan \frac{m\pi}{2}} \quad (4)$$

where  $k$  and  $m$  depend on the metal species.

In 1947 Randles suggested another popular model for electrode-electrolyte interface [4]. In the Randles model, depicted in Fig. 2c, a double-layer capacitance ( $C_d$ ) was added in parallel with a series combination of resistance ( $R$ ) and capacitance ( $C$ ). However, the above mentioned models do not consider the direct current (DC) flowing through the interface. In 1968 [4], Geddes and Baker proposed another model that considers the passage of DC through the interface. In their model the Warburg capacitance is in parallel with the Faradic resistance to model the property of DC that passes through the interface. This model is shown in Fig. 2d.

Moreover, the exchange of the anions and cations at the interface alter the local concentration of cations and anions. Therefore, the neutrality of charge is altered in the solution and makes the electrolyte that is close to the interface a different potential with respect to the rest of the electrolyte, and causes an electric potential difference which is called the half-cell potential. The half-cell potential is related to the metal, the concentration of ions in the electrolyte, temperature and other second-order factors [2]. When a circuit is constructed to allow current to flow across an electrode-electrolyte interface, the observed half-cell potential is often altered. The difference between the observed half-cell potential for a particular circuit and the standard half-cell potential is known as the overpotential. Three basic mechanisms contribute to the overpotential: ohmic, concentration, and activation [2].

Electroencephalography (EEG) is an essential tool for brain and behavioral research. EEG is also one of the mainstays of hospital diagnostic procedures and pre-surgical planning. End users struggle with EEG's poor spatial resolution, selectivity and low signal-to-noise ratio, limiting its effectiveness in research discovery and diagnosis [5]-[6].

Tripolar concentric ring electrodes (TCREs), consisting of three elements including the outer ring, the middle ring,

and the central disc (Fig. 4a, b), are distinctively different from conventional disc electrodes that have a single element (Fig. 3a, b). TCREs have been shown to estimate the surface Laplacian directly [7]. The Laplacian algorithm is two-dimensional and weights the middle ring and central disc signal difference sixteen times greater than the outer ring and central disc signal difference [7]. Compared to EEG with conventional disc electrodes Laplacian EEG using TCREs (tEEG) have been shown to have significantly better spatial selectivity (approximately 2.5 times higher), signal-to-noise ratio (approximately 3.7 times higher), and mutual information (approximately 12 times lower) [8].

In this paper, we developed models for bio-potential electrodes. In particular, we developed mathematical models of our gold-plated TCRE and conventional golden plate cup electrode to compare their properties for biomedical measurements.

## II. PROCEDURE

Fig. 3a illustrates a conventional cup electrode. In order to measure the impedance between two cup electrodes, fresh Ten20 (Weaver and Company) electrode paste was used in each experiment as a skin-to-electrode electrolyte, similar as in real recordings, and to mimic the body. Fig. 3b shows the cup electrodes placed in the Ten20 paste. The equivalent model for this configuration is shown in Fig. 3c. In this model  $R_1$  and  $R_2$  represent the resistivity of the electrodes and  $C_1$  and  $C_2$  are the equivalent double layer capacitor of the electrode-electrolyte interface. The  $R_e$  represents the electrolyte resistance, and the resistances  $R_3$  and  $R_4$  are the equivalent resistors for the leakage current of the electrode electrolyte interface.

Fig. 4a shows the TCRE and with the electrolyte which is depicted in Fig. 4b. Therefore, there is an electrode-electrolyte interface between each pair of rings of the TCRE. Fig. 4c shows part of the electrical model representation for the TCRE electrode-electrolyte interface. (e.g. Middle and Outer elements of the TCRE). The impedance that is seen between the middle ring to the outer ring ( $Z_{mo}$ ) is:

$$Z_{mo} = R_1 + \frac{1}{j\omega C_1} + R_e + \frac{1}{j\omega C_2} + R_2 \quad (5)$$

And the resistive part is:

$$R_{mo} = R_1 + R_e + R_2 \quad (6)$$

where  $R_e$  is an ionic solution resistance that depends on the ionic concentration, types of the ions, temperature and the area in which current is carried. This resistance is defined as:

$$R_e = \rho \frac{L}{A} \quad (7)$$

where  $\rho$  is the solution resistivity. In biomedical applications, it is more common to use the conductivity of the solution. Since the solution conductivity,  $\kappa$ , is the reciprocal of the solution resistivity,  $\rho$ , we can formulate the solution conductivity,  $\kappa$ , as:

$$\kappa = \frac{L}{RA} \quad (8)$$

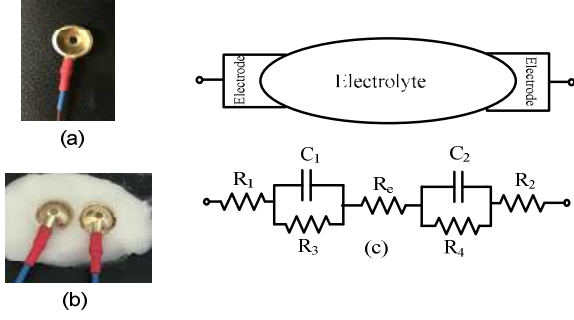


Figure 3: cup electrode (a) cup electrodes placed on Ten20 paste, (b) electrical circuit model of the electrode-electrolyte interface

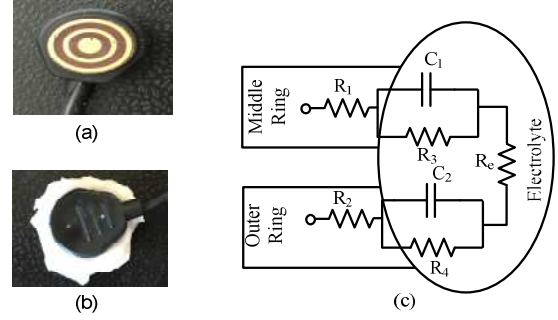


Figure 4: TCRE electrode (a) TCRE placed on Ten20 paste, (b) electrical circuit model of the electrode-electrolyte interface

And the reactive part is:

$$\frac{1}{c_{OD}} = \frac{1}{c_1} + \frac{1}{c_2} \quad (9)$$

Further, to measure the impedance, we performed electrochemical impedance spectroscopy (EIS) using the Gamry potentiostatic instrument framework. We configured the system for two-electrode measurements. In order to measure the impedance between the central disc and middle ring (D-M), we connected the blue (working sense) and green (working current) leads to the middle ring and the white (reference) and red (counter current) leads to the central disc. To measure the impedance between the central disc and outer ring (D-O), we connected the blue and green leads to the outer ring and white and red leads to the central disc. Finally, to measure the impedance between the middle ring and outer ring (M-O), we connected the blue and green leads to the middle ring and the white and red leads to the central disc. The same configuration was used for disc electrodes.

### III. RESULTS

Equation 5 shows that the impedance consists of

capacitance and resistance. Therefore, the impedance changes with the frequency. The Bode plots of the impedances between each pair of rings (D-M, D-O, M-O) of TCRE are shown in Fig. 5a and their Nyquist plots are shown in Fig. 5b. The Bode and Nyquist plots for the cup electrodes are shown in Fig. 6. At low frequencies the cup electrode is more capacitive while the TCRE has a higher impedance in all frequencies. Based on the experimental results and the model parameters studied above, a proposed model for each pair of the tri-polar concentric ring electrode is depicted on Fig. 7.

In order to test the equivalent circuit model, a non-linear least squares fitting program was used to fit the model to the experimental data. The resulting fit with the experimental data for the impedance between the middle and outer rings is depicted in Fig. 5c and Fig 5d, and the parameter values are summarized in Table 1. For a perfect match of the model with the experimental data, a constant phase element (CPE) was used instead of capacitors. This is due to the "double layer capacitors" often behaves like a CPE instead of a pure capacitor [9], [10]. The impedance of a double layer capacitor has the form:

$$Z_{CPE} = \frac{1}{Q(j\omega)^\alpha} \quad (10)$$

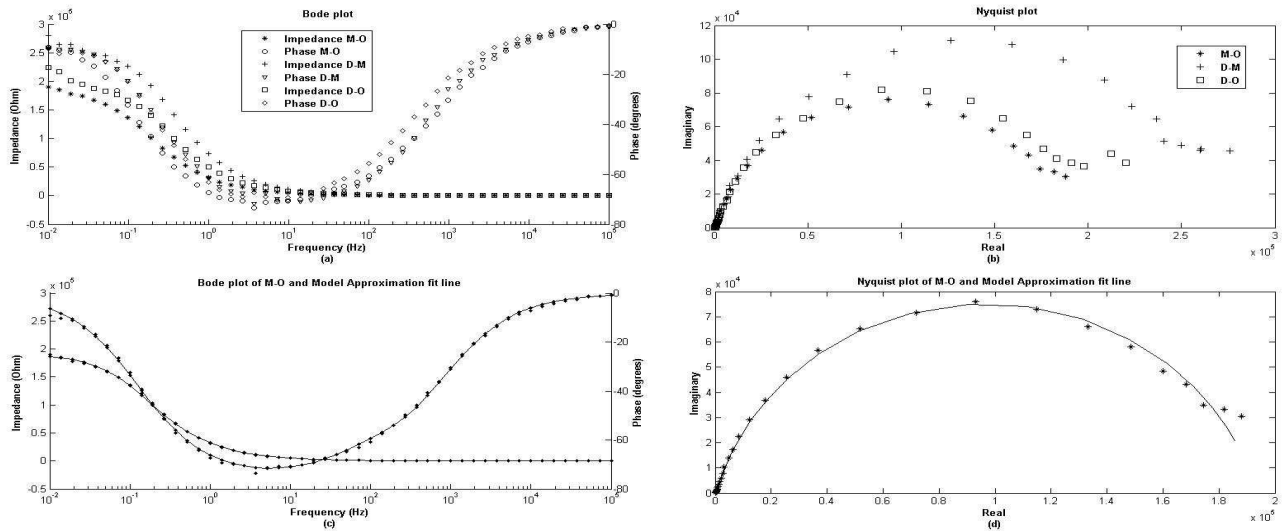


Figure 5: Bode plot of the TCRE (a), Nyquist plot of the TCRE (b), Bode plot of the TCRE with the fitted model (c), Nyquist plot of the TCRE with the fitted model (d)

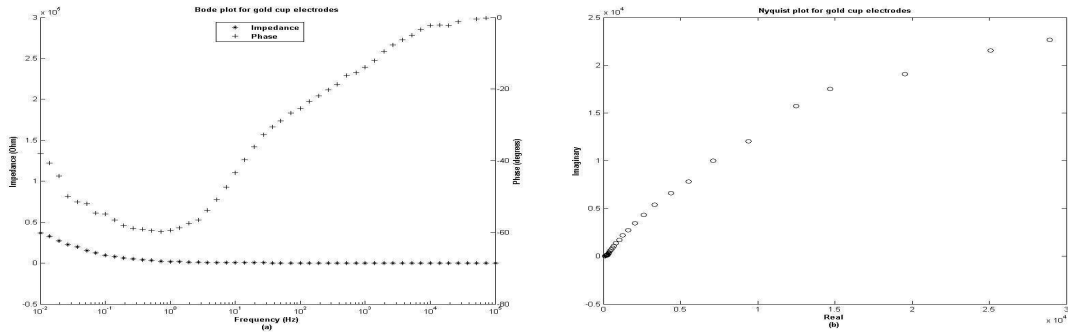


Figure 6: Bode plot of the cup electrode (a), Nyquist plot of the cup electrode (b)

In equation 10, if the constant  $\alpha=1$ , the equation describes capacitance and  $Q$  has units of capacitance. Otherwise, if  $0<\alpha<1$ , the equation represent the CPE and  $Q$  has units of  $Fcm^{-2}s^{(\alpha-1)}$ ,  $\frac{S^\alpha}{\Omega}$ , or  $S \cdot s^\alpha$ . In Table 1 “n” and “m” correspond to the constant  $\alpha$  value of the CPE that is used for the  $C_w$  and  $C_d$  respectively.

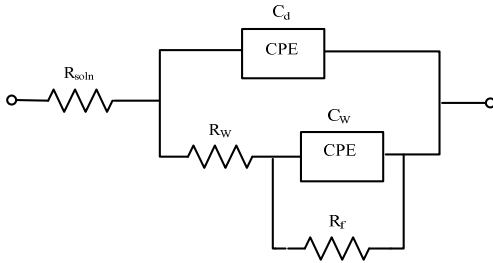


Figure 7: Electrical model for the tri-polar concentric ring electrode

#### IV. CONCLUSION

In this paper, a circuit model for the TCRE and electrode paste was developed and compared to a model for conventional disc electrodes. Observing Figures 5 and 6 there are two items to notice: (1) the TCRE phase only varies from 70 to 60 degrees in the frequency band 1Hz to 100Hz while the cup electrode phase varies from 60 to 25 degrees; and (2) the impedance of the TCRE is below 5 k $\Omega$  from 10Hz and beyond whereas the cup electrode impedance is below 5 k $\Omega$  beyond 0.5 Hz.

Table 1: Parameter values for the tEEG model

Parameters	Value	$\pm$ Error	Units
$R_{soln}$	568.0	5.780	ohms
$R_w$	325.3e3	28.84e3	ohms
$R_f$	82.19e3	24.68e3	ohms
$C_w$	1.553e-6	137.2e-9	$S^*s^\alpha$
$n$	776.6e-3	50.33e-3	
$C_d$	2.081e-6	137.2e-9	$S^*s^\alpha$
$m$	867.4e-3	9.843e-3	

#### ACKNOWLEDGMENT

We would like to thank Dr. Richard Brown for allowing us to use the Gamry potentiostatic instrument framework machine.

#### REFERENCES

- [1] L. A. Geddes, and L. E. Baker, "Principles of applied biomedical instrumentation," (Wiley-Interscience, New York, 1975).
- [2] C. Boccaletti, F. Castrica, G. Fabbri, and M. Santello, "A non-invasive biopotential electrode for the correct detection of bioelectrical currents," In Proceedings of the Sixth IASTED International Conference on Biomedical Engineering, pp. 353-358. ACTA Press, 2008.
- [3] Wang, Hainan, and L. Pilon. "Accurate simulations of electric double layer capacitance of ultra microelectrodes." The Journal of Physical Chemistry C 115, no. 33 (2011): 16711-16719.
- [4] L. A. Geddes, "Historical evolution of circuit models for the electrode-electrolyte interface," Annals of Biomedical Engineering, Vol. 25, pp. 1-14, 1997.
- [5] J. E. Desmedt, V. Chalklinand C. Tomberg, "Emulation of somatosensory evoked potential (SEP) components with the 3-shell head model and the problem of 'ghost potential fields' when using an average reference in brain mapping," Electroenceph. Clin. Neurophysiol., vol. 77, pp. 243-258, 1990.
- [6] P.L. Nunez, R.B. Silberstein, P. J. Cadiush, J. Wijesinghe, A. F. Westdorp, and R. Srinivasan, "A theoretical and experimental study of high resolution EEG based on surface laplacians and cortical imaging," EEG and Clin. Neurophysiology, vol. 90, pp. 40-57, 1994.
- [7] W. Besio, K. Koka, W. Aakula, and W. Dai, "Tri-polar concentric ring electrode development for Laplacian electroencephalography," IEEE Trans Biomed Eng, vol. 53, pp. 926-933, 2006.
- [8] K. Koka and W. Besio, "Improvement of spatial selectivity and decrease of mutual information of tri-polar concentric ring electrodes," J of Neuroscience Methods, vol. 165, pp. 216-222, 2007.
- [9] Chang, Jong-hyeon, Jungil Park, Youngmi Kim Pak, and James Jungho Pak. "Fitting improvement using a new electrical circuit model for the electrode-electrolyte interface." In Neural Engineering, 2007. CNE'07. 3rd International IEEE/EMBS Conference on, pp. 572-574. IEEE, 2007.
- [10] Hirschorn, Bryan, M. E. Orazem, B. Tribollet, V. Vivier, I. Frateur, and M. Musiani. "Constant-phase-element behavior caused by resistivity distributions in films I. Theory." Journal of The Electrochemical Society 157, no. 12 (2010): C452-C457.